Matrix Effect of Alkali and Alkaline Earth Metal Halides on Fluorescence Quantum Yield of Indium in Laser-induced Fluorescence Flame Spectrometry

Ching-Bin Ke (柯清彬) and King-Chuen Lin* (林金全)
Department of Chemistry, National Taiwan University, Taipei 106, and
Institute of Atomic and Molecular Sciences, Academia Sinica, P. O. Box 23-166, Taipei 106, Taiwan, R.O.C.

As interfered with by alkali and alkaline earth metal halides added as the matrix in an acetylene/air flame, the fluorescence quantum yield of In as the analyte in a laser-induced fluorescence (LIF) flame spectrometry has been thoroughly characterized. The fluorescence quantum yield is determined by a ratio of F to A, where F is the measured fluorescence of In and A is the difference between the absorption signals recorded for the analyte and the blank solutions. The normalized fluorescence signal is treated to prevent deviations due to variations of the atomization efficiency under the conditions with and without the matrix added. The fluorescence quantum yield is measured to be almost independent of the matrix concentration up to 500 ppm (μg/mL) studied, under conditions of either optical unsaturation or saturation. By considering a quenching effect induced by electron-atom collisions, the calculated fluorescence quantum yields are consistent with our observations.

INTRODUCTION

The matrix effects on fluorescence and absorption flame and nonflame spectrometric techniques and inductively-coupled plasma (ICP) emission spectrometry have been widely studied. A better understanding of the interference mechanisms involved seems to be crucial to reducing effectively the matrix interference and measuring trace analytes precisely, in addition to optimizing the operating conditions. Essentially the resultant interference may cause such effects as shifting the ionization equlibrium of the analyte,[1,2] inducing chemical reactions,[3,4] varying the properties of analyte volatilization[5,6] and atomization,[7,8] quenching the analyte population in the excited state,[9,10] changing the transport properties of solutions into a flame or an ICP system,[11,12] reforming the spatial distribution of the analyte population,[13,14] causing broadening of the line shape[15,16] and affecting the diffusion of the concentration gradient[17,18] and system temperature.[19,20] The physical and chemical phenomena involved are very complicated and thus the interpretation is very diversified.

Ionization and chemical effects are two interference mechanisms frequently considered in optical flame spectrometry.[1-4] The former process results in a substantial increase in the number of the electrons, which may suppress the ionization of the analyte being detected. On the other hand, the chemical reaction with the matrix added may consume the analyte and thus depress the absorption signal. Several methods, such as chromatographic separation, acidification, and analyte extraction or dilution,[21-24] have been employed to remove or diminish matrix interferences. However, the physical and chemical complexity obscures a detailed understanding of the phenomena involved in most cases. Thus far, research into the matrix effect has been substantially focused on ICP emission and absorption flame spectrometry. LIF flame spectrometry is seldom investigated, especially with regard to the mechanisms that the matrix induces to interfere with the analyte.

In this work, we attempted to understand the matrix effect on the fluorescence quantum yield in LIF flame spectrometry. Alkali and alkaline earth metal halides were used as the matrix and the LIF response of In as the analyte was detected. In addition to causing excitation interference, the matrix effect in LIF may be essentially treated as in the absorption spectrometry. The caused ionization and chemical reactions, considered as the major interferences, may change the atomization efficiency of the analyte. Therefore, the fluorescence quantum yield was treated as a ratio of fluorescence to absorption intensities. The normalized fluorescence becomes independent of the population variation in the ground state of the analyte. In this manner, the fluorescence quantum yield was measured to be almost independent of the matrix studied,

* Corresponding author. Fax: +886-2-23621483; E-mail: kclin@ccms.ntu.edu.tw

under either optical unsaturation or saturation conditions. A theoretical prediction, taking into account the quenching process of electron-atom collisions, is consistent with our observations.

EXPERIMENTAL

Flame System

We performed the LIF and absorption experiments in an atmospheric flame. The apparatus is depicted in Fig. 1. A commercial burner assembly (Perkin-Elmer, Norwalk, CT, USA) with a 100×0.5 mm slot burner head was coupled with an interlocked gas control system, by means of which acetylene and air were premixed prior to reaching the burner head. The flow rate of the fuel and the air were regulated at 0.5 L/min and 12.5 L/min, respectively. The flame temperature was previously determined to be 2500 K.[25,26] Aqueous solutions of In salt were prepared from 1 to 100 ppm (μg/mL) and nebulized at a flow rate of 4.5 mL/min into the burner head.

Laser Source

The light source for LIF detection was a 10 Hz, 5-8 ns Nd:YAG laser-pumped dye laser (Quanta Ray PDL-2, CA, USA), emitting at 651.2 nm with the use of a DCM dye. The radiation was then frequency-doubled through a KDP crystal which was housed in a wavelength extender with a device of auto-tracking controller (Quanta Ray WEX, CA, USA). The resulting wavelength at 325.6 nm was used to excite the In atom in the $5^2P_{3/2} \rightarrow 5^2D_{5/2}$ transition. The unfocused excitation beam was collimated with a pinhole of 5 mm^2 cross section and then directed longitudinally through the flame at 12 ± 0.1 mm above the burner head. The laser energy, prior to reaching the flame, was measured continuously by a surface absorbing disk calorimeter (Scientech 36-0001, CO, USA).

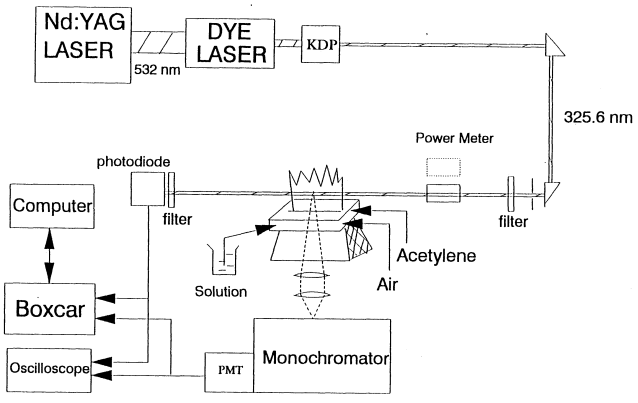

Fig. 1. Schematic diagram of the apparatus for laser-induced fluorescence and atomic absorption detection.

Reagents

Analytical-reagent grade salts (Merck, Darmstadt, Germany) were used to prepare the analyte and matrix solutions. For most experiments, the analyte was prepared at a 3 ppm In concentration, which lay in the linear range in the concentration dependence measurements. The matrix solutions of alkali and alkaline earth metal chlorides (LiCl, NaCl, RbCl, CsCl, $MgCl_2$, $CaCl_2$, $SrCl_2$, and $BaCl_2$) were prepared at metal concentrations of 500 ppm.

Nebulization Efficiency Measurement

We measured the nebulization efficiency to be 0.090 ± 0.006 for the analyte under the conditions with and without 500 ppm of interferents. This rules out nebulization and transport as important contributors to the observed matrix behavior. A similar conclusion was reached in ICP experiments.[13]

LIF and Absorption Detection

The non-resonance fluorescence in the $6^2S_{1/2} \rightarrow 5^2P_{1/2}$ transition at 410.1 nm was monitored, as In was excited from the $5^2P_{3/2}$ to the $5^2D_{5/2}$ state. The signal was collected perpendicularly relative to the laser beam axis onto a monochromator (McPherson 270, MA, USA) via a pair of lenses of 10 and 2.5 in. The entrance and the exit slits of the monochromator were open to 500 μm; the grating was set at 410.1 nm, allowing for a spectral transmittance of 1 nm. The transmitted LIF was detected by a photomultiplier tube (Hamamatsu R955, Hamamatsu City, Japan) attached to the monochromator, and fed into a boxcar integrator (EG&G PAR Models 4402 and 4422, Princeton, NJ, USA) for improvement of the signal-to-noise ratio. The data was then stored in a microcomputer for further treatment.

The absorption spectrum of the analyte In was detected with a photodiode, which was positioned along the laser beam axis. For optimizing the instrument sensitivity and avoiding any optical saturation, the power of the incident laser beam was appropriately attenuated using the filters. The experimental conditions were otherwise identical with those for the LIF apparatus.

Experimental Conditions

A partial energy diagram of the In atom for non-resonance LIF detection is shown in Fig. 2. The initial state $5^2P_{3/2}$, with an energy 2213 cm^{-1} above the ground state $5^2P_{1/2}$, was thermally populated. A careful test was made to

ensure accurate detection of the signal. A linear dynamic range of the In concentration was measured up to 100 ppm. A 3 ppm In concentration was accordingly used throughout the experiments. The dependence of the LIF signal on the laser power for a 3 ppm In solution was measured. The background response was determined as the laser was detuned off the resonance line, assuming that the interference by the scattered radiation was independent of the laser wavelength. Under the conditions used, the fluorescence signal became optically saturated when the laser energy exceeded 100 μJ. Two parallel experiments for the matrix effect on unsaturated and saturated LIF were conducted simultaneously. The corresponding incident laser energy was maintained at 60 ± 3 μJ and 300 ± 15 μJ, respectively.

RESULTS AND DISCUSSION

Measurements of fluorescence, absorption and quantum yield

Based on the apparatus described earlier, LIF and absorption spectra of 3 ppm In with and without matrix added were measured. The fluorescence quantum yield is proportional to the ratio of F to A, where F is the measured fluorescence of In and A is the difference between the absorption signals recorded for the analyte and the blank solutions.[9,27] The absorption measurement reflects the relative ground state population of the analyte under the conditions with and without the matrix added.

To justify the matrix effect on the fluorescence quantum yield, a ratio

$$\frac{Y_{MX}}{Y} = \frac{F_{MX} / A_{MX}}{F / A} \quad (1)$$

is written, where F_{MX} and A_{MX} denote the quantities measured when various types of Group 1A and 2A metal chlorides were added along with the analyte solution. The relative unsaturation fluorescence, F_{MX}/F, and relative absorption measurement, A_{MX}/A, are shown in Fig. 3, where 500 ppm of each metal-containing matrix were added. The corresponding relative quantum yield, as expressed by eq. 1, is shown in Fig. 4. The saturation fluorescence radiance was verified to depend on the total atomic population density and the spontaneous emission coefficient of the excited state analyte of interest.[28] That is, under the saturation conditions excitation interference can be neglected and only atomization interference will be considered. In fact, the measured relative quantum yield, Y_{MX}/Y, appears to be independent of the alkali and alkaline earth metal chlorides added, under either unsaturation or saturation conditions. Our results show an insignificant difference between these two optical conditions, as the matrix concentration is at 500 ppm, larger than the analyte concentration by about two orders of magnitude. However, the upper limit of matrix concentration that does not affect the fluorescence quantum yield has not been determined.

In the fluorescence measurement, In is excited via the $5^2P_{3/2} \rightarrow 5^2D_{5/2}$ transition, while the LIF is monitored at 410.1

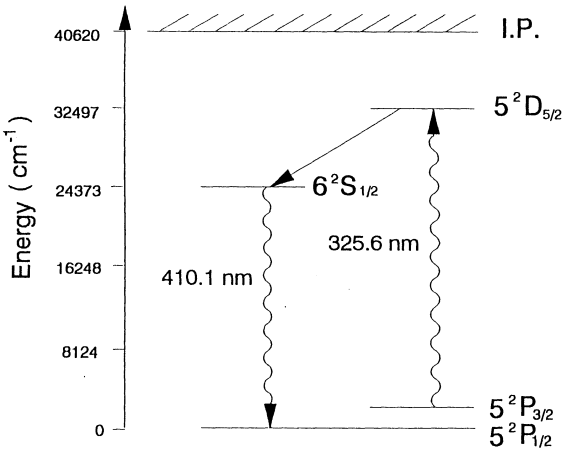

Fig. 2. Partial energy diagram of the In atom for the non-resonance LIF detection for $6^2S_{1/2} \rightarrow 5^2P_{1/2}$ emission with $5^2P_{3/2} \rightarrow 5^2D_{5/2}$ excitation. The $5^2D_{5/2} \rightarrow 6^2S_{1/2}$ transition is activated by collisions.

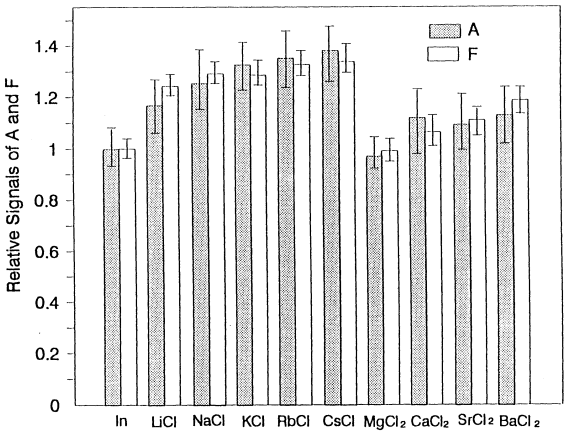

Fig. 3. Matrix dependence of unsaturation fluorescence, F, and absorption, A, measurement of a 3 ppm In solution. The absorption is expressed by the difference in signals recorded for the analyte and the blank solution. The F and A measurements are normalized to the signals of In in the absence of matrix. The alkali and alkaline earth metal chlorides were prepared at a 500 ppm metal concentration.

nm from the $6^2S_{1/2}$ to $5^2P_{1/2}$ state. The $6^2S_{1/2}$ state is populated via collisional deactivation. The collisional deactivation rate stemming from the $5^2D_{5/2}$ state may be dominated by the $5^2D_{5/2}$-$6^2S_{1/2}$ transition, with energy difference of ~ 8000 cm^{-1}, due to the effect of near resonance energy transfer. The fraction of $5^2D_{5/2}$-$6^2S_{1/2}$ energy transfer may not be affected by the addition of matrix, of which the concentration is negligible as compared to the condition of 1 atm flame compositions. Our observation of the relative quantum yield, Y_{MX}/Y, also shows that the matrix effect on the collisional deactivation in the $5^2D_{5/2} \rightarrow 6^2S_{1/2}$ transition should be negligible.

As salt matrix interferent is added to the In solution, several possible disturbances may occur. First, the released alkali or alkaline earth metals have a relatively low ionization potential, thus feasibly inducing the ionization process in the flame. Through the mass action effect, the excess of electrons released may shift the ionization equilibrium of the analyte, thereby suppressing the In ionization reaction.[1,2,29] In this sense, the LIF signal of the analyte will be enhanced owing to the increase in the neutral In atoms available for excitation. Second, the released non-metal atoms may lead to a chemical reaction with the analyte to form an indium monohalide compound, which causes suppression of the LIF signal.[3,4,30,31] Third, the matrix itself or the released species, including the electrons, may interfere with the excited state of In, thereby enhancing the radiationless collisional deactivation.[9,10,32] In this work, the normalized fluorescence signal is treated to prevent deviations due to variations of the atomization efficiency under the conditions with and without the matrix added.

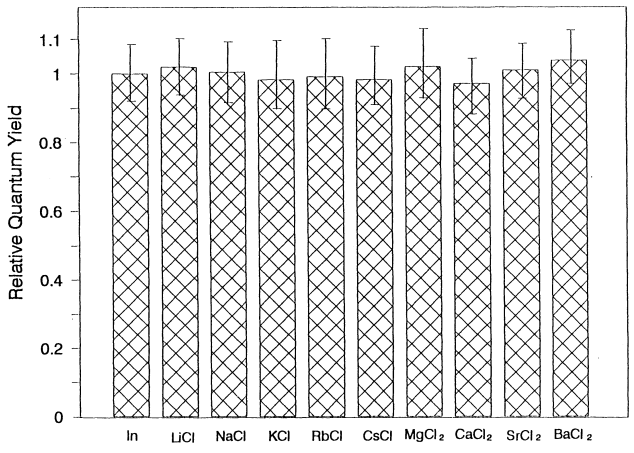

Fig. 4. Relative quantum yield of fluorescence measurement for a 3 ppm In solution as a function of matrix. The alkali and alkaline earth metal chlorides were prepared at a 500 ppm metal concentration.

Theoretical prediction of relative quantum yield

For comparison with our observations, the fluorescence quantum yield is estimated theoretically. As in the ICP-emission spectrometry,[9,32] the electron-impact collisions are considered to be the major contributor to the collisional deactivation processes in the LIF flame spectrometry. Assuming that the electron velocity follows a Maxwellian distribution and the microscopic reversibility holds for the quenching collision, one obtains the quenching rate coefficient, k_q, for the electron-impact collision:[9,32]

$$k_q = (g_o / g_1)\sigma_e\left(1+\frac{E_{ex}}{kT}\right)\sqrt{\frac{8kT}{\pi m_e}} \qquad (2)$$

where g_o and g_1 are the statistical weights for the ground and the excited states of In, respectively, m_e is the electron mass, k is the Boltzmann constant, T is the system temperature, and σ_e is the electron-impact excitation cross section as the electron energy is above the excitation threshold, E_{ex}.[33] By taking into account a flame temperature of 2500 K, an average relative velocity of the electron of 3.1×10^7 cm s^{-1} and the related cross section 1 $Å^2$, according to eq. 2, the rate coefficient of electron-atom collisions is estimated to be 3.1×10^{-9} cm^3 s^{-1}, only an order of magnitude smaller than in ICP. Note that the cross section adopted here is 3-6 times larger than those ever reported for different transitions.[34]

Given the electron number density, n_e, the radiative lifetime, τ_o, of the excited state and the quenching rate coefficient of electron-atom collisions, the quantum yield, Y, may be calculated as follows:[9,32]

$$Y = \left[1+\tau_o n_e (g_o / g_1)\sigma_e\left(1+\frac{E_{ex}}{kT}\right)\sqrt{\frac{8kT}{\pi m_e}}\right]^{-1} \qquad (3)$$

Among those parameters required, the electron number density may be determined from the equilibrium constant for flame ionization. According to the Saha equation, this ionization equilibrium constant for the analyte or the matrix in the flame can be expressed in terms of the related partition function by[33]

$$K_i = \frac{n_{A^+} n_e}{n_A} = \frac{(2\pi m_e kT)^{3/2}}{h^3}\frac{2Q_i}{Q_A}\exp(-V_i / kT) \qquad (4)$$

where n_A, n_{A+}, and n_e denote the number densities of atoms, ions and electrons, respectively, h is the Planck's constant, Q_i and Q_A are the electronic partition function of the ion and the atom, respectively, and V_i is the ionization potential. The ion temperature is considered to be equal to the electron temperature under the conditions of thermal equilibrium. The value

Table 1. Calculated Ionization Equilibrium Constants K_i, Ionization Potentials (I.P.), and Atomization Efficiencies ε, for Alkali, Alkaline Earth Metals and the Analyte In

Metal	K_i	I.P. (eV)	ε[a]
Li	4.05×10^9	5.39	0.2
Na	1.30×10^{10}	5.13	1
K	5.33×10^{10}	4.34	0.3
Rb	1.13×10^{12}	4.17	0.6
Cs	4.23×10^{12}	3.89	0.73
In	4.04×10^9	5.78	0.67
Mg	4.58×10^5	7.64	1
Ca	5.66×10^8	6.11	0.06
Sr	3.96×10^9	5.69	0.1
Ba	3.73×10^{10}	5.21	0.0034

[a] Ref. 37, 38.

of Q_i/Q_A is estimated to be 0.32, 0.5 and 2 for indium, alkali metal, and alkaline earth metal, respectively.[35] Substituting into eq. 4 the ratio, the electron mass, a known flame temperature, and the relevant ionization potential, the respective ionization equilibrium constant for the analyte and the metal matrix can be obtained. The results are given in Table 1. The value of n_e may be subsequently evaluated under the conditions with and without the matrix added, provided that n_A is known. n_A may be estimated by the product of the atomization efficiency and the total number density of the element A in the flame, which can be readily determined in terms of the solution concentration.[36] The atomization efficiencies for indium, alkali metal, and the alkaline earth metal are referred to in references.[37,38] Their values are also listed in Table 1.

Substituting into eq. 3 the quenching rate coefficient of electron-atom collisions, the radiative lifetime of 7.69 ns for the In $5^2D_{5/2}$ state and the electron number density of 8.3×10^{11} cm^{-3} and 2.9×10^{10} cm^{-3} evaluated with and without addition of 500 ppm matrix (NaCl as an example), respectively, the values of Y_{NaCl} and Y are predicted to be 0.99975 and 0.99999, respectively. Analogously, we estimated the electron quenching rate coefficient related to the In $6^2S_{1/2}$ state, and in turn obtained fluorescence quantum yields of 0.99970 and 0.99999 with and without addition of NaCl, respectively. The quantum yield for the non-resonance LIF in a flame system is verified to be independent of the studied concentration of the Group 1A and 2A metal halides as the matrix. This conclusion is consistent with the observations.

Note that the theoretical prediction involves several assumptions, such as neglect of the quenching process by the species other than electrons, neglect of three-body collisions, validity of local thermal equilibrium for the electron velocity distribution and validity of microscopic reversibility. As with ICP, the electrons produced in a flame have a relatively large number and a substantial collisional cross section interacting with the analyte. The electron number density of 8.3×10^{11} cm^{-3} is roughly 1-2 orders of magnitude smaller than the total number density of matrix nebulized. However, the collision cross section by electrons is 2-3 orders of magnitude larger than that by most atomic species released. It is reasonable to assume that the electron-atom collision is predominantly responsible for the quenching process. The other assumptions described above have been widely adopted in flame and ICP systems.[9,32]

CONCLUSION

We have studied the fluorescence quantum yield of In as interfered with by Group 1A and 2A metal chlorides in an acetylene/air flame. A normalized fluorescence of In was measured to characterize the fluorescence quantum yield, for preventing population variation of ground state In atoms caused by the addition of the metal chlorides. The measured fluorescence quantum yield was almost independent of the matrix concentration studied, under either optical unsaturation or saturation conditions. The theoretical prediction, involving the quenching process of electron-atom collisions, agrees with the observations.

ACKNOWLEDGMENT

This work is financially supported by the National Science Council of the Republic of China under the contract no.NSC 89-2119-M-002-007.

Received January 28, 2002.

Key Words

Matrix effect; Fluorescence quantum yield; Laser-induced fluorescence.

REFERENCES

1. Luecke, W. *Spectrochim. Acta* **1992**, *47B*, 741.
2. Grove, E. L.; Scott, C. W.; Jones, F. *Talanta* **1965**, *12*, 327.
3. Haraguchi, H.; Fuwa, K. *Spectrochim. Acta* **1975**, *30B*, 535.
4. Kantor, T. *Spectrochim. Acta* **1994**, *49B*, 1717 and 1733.

5. Kantor, T.; Bezur, L.; Pungor, E.; Winefordner, J. D. *Spectrochim. Acta* **1983**, *38B*, 581.
6. Fuller, C. W. *Anal. Chim. Acta* **1976**, *81*, 199.
7. Olivares, J. A.; Houk, R. S. *Anal. Chem.* **1986**, *58*, 20.
8. Hobbs, S. E.; Olesik, J. W. *Appl. Spectrosc.* **1991**, *45*, 1395.
9. Wu, M.; Hieftje, G. M. *Spectrochim. Acta* **1994**, *49B*, 149.
10. Omenetto, N. *Spectrochim. Acta* **1988**, *43B*, 63.
11. Skogerboe, R. K.; Olson, K. W. *Appl. Spectrosc.* **1978**, *32*, 181.
12. Borowiec, J. A.; Boom, A. W.; Dillard, J. H.; Cresser, M. S.; Browner, R. F.; Matteson, M. J. *Anal. Chem.* **1980**, *52*, 1054.
13. Rybarczyk, J. P.; Jester, C. P.; Yates, D. A.; Koirtyohann, S. R. *Anal. Chem.* **1982**, *54*, 2162.
14. Kornblum, G. R.; De Galan, L. *Spectrochim. Acta* **1977**, *32B*, 445.
15. Boss, C. B.; Hieftje, G. M. *Anal. Chem.* **1979**, *51*, 895.
16. West, A. C.; Fassel, V. A.; Kniseley, R. N. *Anal. Chem.* **1973**, *45*, 2420.
17. Blades, M. W.; Holick, G. *Spectrochim. Acta* **1981**, *36B*, 861.
18. Galley, P. J.; Glick, M.; Hieftje, G. M. *Spectrochim. Acta* **1993**, *48B*, 769.
19. Gunter, W. H.; Visser, K.; Zeeman, P. B. *Spectrochim. Acta* **1982**, *37B*, 571.
20. Caughlin, B. L.; Blades, M. W. *Spectrochim. Acta* **1985**, *40B*, 987.
21. Bolshov, M. A.; Zybin, A. V.; Koloshnikov, V. G.; Smirenkina, I. I. *Spectrochim. Acta* **1988**, *43B*, 519.
22. Jackson, K. W.; Mahmood, T. M. *Anal.Chem.* **1994**, *66*, 252R.
23. Kachin, S. V.; Smith, B. W.; Wineforder, J. D. *Appl. Spectrosc.* **1985**, *39*, 587.
24. Fang, Z.; Dong, L.; Xu, S. *J. Anal. At. Spectrom.* **1992**, *7*, 293.
25. Su, K. D.; Chen, C. Y.; Lin, K. C.; Luh, W. T. *Appl. Spectrosc.* **1991**, *45*, 1340.
26. Ke, C. B.; Lin, K. C. *Appl. Spectrosc*. **1998**, *52*, 187.
27. Pearce, S. J.; De Galan, L.; Winefordner, J. D. *Spectrochim. Acta* **1968**, *23B*, 793.
28. Winefordner, J. D. *J. Chem. Educ.* **1978**, *55*, 72.
29. Gilmutdinov, A. Kh.; Shlyachtina, O. M. *Spectrochim. Acta* **1991**, *46B*, 1121.
30. Fujiwara, K.; Haraguchi, H.; Fuwa, K. *Anal. Chem.* **1975**, *47*, 1670.
31. Haraguchi, H.; Fuwa, K. *Bull. Chem. Soc. Japan.* **1975**, *48*, 3056.
32. Hasegawa, T.; Smith, B. W.; Winefordner, J. D. *Spectrochim. Acta* **1987**, *42B*, 1093.
33. Alkemade, C. Th. J.; Hollander, T. J.; Snelleman, W.; Zeegers, P. J. Th. *Metal Vapors in Flames*; Pergamon Press: Oxford, 1982; pp 13-90 (ch.2); pp 460-461 (ch.4).
34. Nepiipov, E. I. *Opt. Spectrosc.* **1975**, *38*, 186.
35. De Galan, L.; Smith, R.; Winefordner, J. D. *Spectrochim. Acta* **1968**, *23B*, 521.
36. Winefordner, J. D.; Vickers, T. J. *Anal. Chem.* **1964**, *36*, 1939.
37. De Galan, L.; Winefordner, J. D. *J. Quant. Spectrosc. Radiat. Transfer.* **1967**, *7*, 251.
38. De Galan, L.; Samaey, G. F. *Spectrochim. Acta* **1970**, *25B*, 245.